Talanta 252 (2023) 123779

Contents lists available at ScienceDirect

Talanta

journal homepage: www.elsevier.com/locate/talanta

A rapid capillary-channeled polymer (C-CP) fiber spin-down tip approach for the isolation of plant-derived extracellular vesicles (PDEVs) from 20 common fruit and vegetable sources

Kaylan K. Jackson [a], Carolina Mata [b], R. Kenneth Marcus [a,*]

[a] Clemson University, Department of Chemistry, Clemson, SC, 29634, USA
[b] California State Polytechnic University, Pomona, CA, USA

ARTICLE INFO

Keywords:
Plant-derived extracellular vesicles (PDEVs)
Exosomes
Plant materials
Isolation
Capillary-channeled polymer (C-CP)
Solid-phase extraction (SPE)

ABSTRACT

In the emerging field of phyto-nanotechnology, 30–200 nm plant-derived extracellular vesicles (PDEVs) are now known to contain active biomolecules that mediate cell-to-cell communication processes in a manner very similar to exosomes in mammalian cells. The ability to deliver cargo across cellular membranes suggests that botanical systems could be used in the mass production of therapeutic vectors to transport exogenous molecules into human cells. The fundamental biochemical characteristics of PDEVs remain poorly understood due to the lack of efficient methods to isolate and characterize these nanovesicles. Described here is a rapid PDEV isolation method using a hydrophobic interaction chromatography (HIC)-based extraction performed on a capillary-channeled polymer (C-CP) fiber spin-down tip. The C-CP solid-phase extraction method is performed using a standard table-top centrifuge, enabling the isolation and concentration of PDEVs (>1 × 10^{10} particles from 100 μL of sample). PDEVs of 189 nm average diameter were obtained from 20 common fruit and vegetable stocks. The size, integrity, and purity of the recovered PDEVs were assessed using transmission electron microscopy (TEM), multi-angle light scattering (MALS), absorbance quantification, a protein purity assay, and an enzyme-linked immunosorbent assay (ELISA) to the PEN1 PDEV surface marker protein. The HIC C-CP tip isolation method allows for concentrated PDEV recoveries (up to 2 × 10^{11} EVs) on reasonable time scales (<15 min) and low cost (<$1), with the purity and integrity fit for fundamental research and downstream applications.

1. Introduction

In many organisms, intercellular communication processes are facilitated by nanometer-scale extracellular vesicles (EVs), which contain host cell-specific proteins, lipids, and genetic content (e.g. DNA, RNA, miRNA) [1,2]. To date, much of EV research has been performed using EVs sourced from human patient biofluid samples or cell culture media to assess the critical roles these vesicles play in signaling and disease progression [3–5]. Scientists have also suggested the therapeutic application of exosomes (30–200 nm EV), where the strategic delivery of drug and gene therapies is allowed [6–8]. With this, a growing body of literature has revealed that several non-human cell sources produce nanovesicles that display many exosome-characteristic structural and functional features [1,2]. Exosome-like vesicles have been discovered in all three domains of life, including species such as bacteria (outer-membrane vesicles, OMVs) [9,10], fungi [11,12], parasites [13], and plants [11,14–17]. Though the nanovesicles from *all* sources remain poorly understood, researchers have suggested the use of plant-derived extracellular vesicles (PDEVs) in therapeutic applications because of the roles they play in the transport of bioactive molecules from plants to human cells [16,18].

PDEVs may be promising candidates for use as therapeutic delivery vectors because of their non-immunogenic traits and potentially cost-effective production from natural renewable sources [19]. The first examples of PDEVs were identified in wheat-sourced mesophyll cells by Shaw et al. [20] and carrot sample stocks by Jensen et al. [21] in the 1960s, even before human-sourced “exosomes” were identified. During the initial PDEV assessment using electron microscopy, the EV-characteristic size and structural features were revealed, though not fully appreciated due in part to the recent emphasis on mammalian EV research [20]. Continued works have confirmed these initial findings and have shown that PDEVs, like human-sourced EVs, contain a

* Corresponding author.
E-mail address: marcusr@clemson.edu (R.K. Marcus).

https://doi.org/10.1016/j.talanta.2022.123779
Received 18 May 2022; Received in revised form 18 July 2022; Accepted 24 July 2022
Available online 13 August 2022

cell-derived lipid bilayer membrane and miRNAs, mRNAs, proteins, lipids, and metabolites from the originating plant cell [22]. Further, works by Zhang et al. [23] have demonstrated that the PDEVs obtained from common edible plant sources are actively endocytosed by macrophages and intestinal stem cells and are able to activate signaling pathways in murine (mice) cells.

Though little is known about the biogenesis, uptake, release, composition, function, and stability of PDEVs relative to their mammalian counterparts [16], it is known that PDEVs contain specific surface marker proteins that are incorporated through the biogenesis process such as Penetration 1 (PEN1) or Syntaxin 121 (SYP121) [24–28]. Though there are some differences in function, the PEN1 protein seems to serve a similar role to that of tetraspanin proteins (i.e., CD9, CD81, CD63) in human-sourced EVs for vesicle identification purposes. The PEN1 protein generically functions as a positioning anchor for the KAT1 K+ channel protein on the plasma membrane and is involved in biological processes such as endo- and *exo*-cytosis, intracellular protein transport, and vesicle docking and fusion [25]. Likewise, the PEN1 protein has been previously found in high concentrations when PDEVs are present and have allowed for the identification of PDEVs based on PEN1 protein detection via immunoassays.

Regardless of the many promising applications of PDEVs (and EVs of all origins), the exact mechanisms of these interactions are largely unknown and require additional investigation. A recent review by Rutter and Innes succinctly reviewed the state of the art and challenges in PDEV research [18]. Additionally, much work is needed to standardize the processing and characterization of PDEVs before their full implementational impacts can be realized [16,29]. One of the primary limiting factors to understanding PDEV fundamentals is the lack of methods for the isolation of these vesicles. Several studies have demonstrated that PDEVs may be isolated from various parts of plants, including plant juices [30–32], roots [33,34], seeds [35,36], and dried plant materials [37]. Most commonly, fluids from these sample types are obtained through a blending/homogenization process and then applied to standard EV isolation protocols (i.e., ultracentrifugation, UC). Though multiple techniques are available for the isolation of EVs from mammalian sources, the majority of published works have reported the use of the ultracentrifugation (UC) method for PDEV sample processing [19,22]. But as seen with human EVs, the UC method is likely to produce PDEV recoveries that are compromised by concomitant matrix species and low yields [38–40], particularly in regards to further bio-characterization such as mass spectrometric proteomics [41,42]. Overall, the available isolation methods do not yield the concentration and purity of EVs needed for fundamental research, much less therapeutic applications [18,19,43]. Hence, the introduction of an isolation method to provide highly pure, concentrated, and functionally-preserved collections of PDEVs is necessary for fundamental research as well as therapeutic vector applications.

As the potential pitfalls in mammalian exosome isolation are well known, there are two primary sources of error/contamination in PDEV isolation. The first, is a high possibility that the populations included in extracts are co-inclusive of vesicles both of extracellular origin and endosomal vesicles which were released due to the destruction of cellular membranes during homogenization, i.e., truly not extracellular. As an alternative to this destructive sample preparation method, Innes et al. [15,17,18,27,44,45] have developed a protocol for non-destructive PDEV harvest through the collection of apoplastic wash from *Arabidopsis thaliana* plants, where these plant biofluids are employed in UC protocols to obtain PDEVs of true extracellular origin [27]. The second source of non-targeted vesicles is the due to possible carryover of EVs originating from plant material having bacteria of various sorts on their surface. Works by Gourabathini et al. have revealed the presence of bacterial pathogens in high concentrations in stocks obtained from local grocery stores [46]. These pathogens expel vesicles that settle on vegetable leaves [9,10,47]. While these EVs would certainly have different surface and cargo makeup from the PDEVs, their presence would certainly bear on the EV purity and the results of fundamental studies. Eventually, all proposed methods of PDEV recovery and use must address these potential challenges.

Ongoing work by Marcus and colleagues has produced a novel EV isolation method based on hydrophobic interaction chromatography (HIC) via a polyester (PET) capillary-channeled polymer (C-CP) fiber stationary phase [48–52]. The C-CP phase consists of melt-extruded fibers with an 8-legged peripheral shape, creating single-micron sized channels when packed into a column format. The relative hydrophobicity of the PET C-CP phase and gentle HIC solvent system allows for effective, vesicle-preserving EV isolations to be performed, where a high-to-low salt solvent transition drives the capture and subsequent release of EVs. The straightforward and cost-effective HIC C-CP method was first performed using a traditional HPLC workflow, where the simultaneous isolation and quantification of EVs was allowed using on-line absorbance (scattering) detection [48–50,52]. More recently, the method has been adapted to a clinically practical solid-phase extraction (SPE) spin-down tip format, where the batch processing of EVs is only limited by the capacity of the table-top centrifuge [51,53,54]. The C-CP spin-down tip method has demonstrated the ability to produce highly concentrated (up to 1×10^{12} particles mL^{-1}), high-purity (>90% removal of protein/lipoprotein contaminants), and bioactive EV recoveries from a plethora of biofluids in less than 15 min [51,54–56]. Indeed, the fiber-based isolation method compares very favorably with other methodologies [56], including the area of mass spectrometric proteomics [57].

Here, the capabilities of the fiber spin-down tip method for the isolation of PDEVs from various plant sample stocks is explored. The recovered PDEVs are evaluated using absorbance (scattering) quantification, multi-angle light scattering (MALS) sizing, and transmission electron microscopy (TEM) imaging. The purity of the PDEVs was assessed using a Bradford assay based on the removal of unwanted free/matrix proteins. The identity of the PDEVs is confirmed using antibodies to the aforementioned PEN1 protein via an indirect enzyme-linked immunosorbent assay (ELISA), allowing differentiation from bacteria-originating EVs. The methodology presented here addresses many of the limitations in PDEV isolation which have hindered their fundamental research and downstream application.

2. Materials and methods

2.1. Chemicals and reagents

Deionized water (DI-H_2O, 18.2 MΩ cm) was obtained from a Milli-Q water purification system (Millipore Sigma, Merck, Darmstadt, Germany). Biotechnology-grade glycerol and ammonium sulfate were purchased from VWR (Sokon, OH, USA). Phosphate buffered saline (PBS, pH = 7.4), bovine serum albumin (BSA), and Pierce™ Coomassie Plus (Bradford) Assay Reagent were purchased from ThermoFisher Scientific (Waltham, MA, USA).

2.2. Instrumentation

A NanoVue Plus UV–Vis spectrophotometer (GE Healthcare, Chicago, IL, USA) was used during the PDEV absorbance quantification (203 nm). The DAWN multi-angle light scattering (MALS) detector (Wyatt Technology, Goleta, CA, USA) was used for size determination efforts. A Synergy H1 Hybrid Multi-Mode Plate Reader (BioTek, Winooski, VT, USA) was used to measure the UV–Vis absorbance (595 nm) of samples in the 96 cell-well format, where the colorimetric Pierce™ Coomassie Plus (Bradford) Assay Reagent was used for Bradford assay detection. The Hitachi HT7830 transmission electron microscope (Chiyoda City, Tokyo, Japan) was used for TEM imaging for EV visualization and structural characterizations.

2.3. Extracellular vesicle sources

While certified EVs from plant-based sources would be a key element in evaluating new methods of PDEV isolation, no such materials are commercially available. As such, the closest approximation is the use of EV materials of different sources, which have the same nominal physico-chemical makeup. Exosomes employed during the quantification work were sourced from a commercial lyophilized stock from HEK293 cell culture media by HansaBioMed (Tallinn, Estonia). To clarify, the EVs employed here are not a standardized EV reference material, and with this, no purity or classification metrics were supplied by the manufacturer. However, the product does serve as an EV source of known concentration (2.7×10^{12} particles mL^{-1}). Concerns regarding the size (including EVs of <30 nm and >200 nm diameter) and purity (the absence of contaminant matrix species like lipoproteins and other protein contaminants) of the exosomes included in these materials have previously been expressed [54], and their potential contributions to systematic error is acknowledged here.

The raw fruits and vegetables used in this study were obtained from the produce section of the local Walmart (Central, SC, USA). The produce stocks included in this study were loosely categorized by type: leafy greens (represented in green font in data sets), vegetables (represented in red), and fruit (represented in blue). Shown in Table 1 are the plant samples in each category, along with the scientific name of each plant. If PDEVs from the presented sample stock have been previously identified in the literature, the size of PDEVs obtained from each, and the employed isolation method used to obtain such, are also presented in the Table.

The raw plant samples were first rinsed with DI water, then chopped into manageable portions, placed into a weighing boat, and weighed using a standard analytical scale. For the solid plant samples, 10 mL of Milli-Q water was added, then the sample was placed in a Magic Bullet™ (Homeland Housewares, Los Angeles, CA) blender and blended until a homogeneous liquid was obtained. For the difficult-to-blend samples (ginger, cilantro, carrots, and strawberry), a mortar and pestle were used for further sample homogenization. The resulting fluid from each sample was aspirated using a sterile, 3 mL single-use syringe (with a 21 G x 1 1/2 in. needle attached; BD, Franklin Lakes, NJ), then filtered using a 0.22 μm PES syringe filter. Finally, 100 μL of the filtered fluid from each sample was processed through the C-CP tip isolation workflow. A visual representation of the sample preparation process is presented in Fig. 1. For the already-liquid samples included here (aloe vera juice and lemon juice), the samples were filtered using a 0.22 μm PES syringe filter before C-CP tip processing.

2.4. C-CP fiber spin down tip assembly and sample processing

The C-CP fiber SPE spin-down tips were assembled following the previously reported protocols, and the same HIC isolation workflow was performed [51,54]. To summarize, 1 cm C-CP fiber-packed tips (with an additional 0.5 cm of void space for attachment) were cut from a 30 cm long, 0.8 mm inner diameter fluorinated ethylene–propylene (FEP) C-CP packed columns consisting of 456 individual PET C-CP fibers to create an interstitial fraction of ~0.6, and bed volume of ~3 μL. The 1.5-cm C-CP fiber-packed tips were press-fit to the narrow end of a 200 μL low retention micropipette tip and held in place using a small amount of liquid adhesive around the periphery of the 200 μL tip.

The PDEV isolations were performed as previously described [51, 54]. After sample processing, 100 μL of the resultant filtered plant supernatant was mixed with 100 μL of ammonium sulfate (2 M final concentration) and deposited inside the sample reservoir of the C-CP tip. The C-CP tip was secured into a 15 mL conical tube using a tip-modified conical adapter cap, then placed inside the table-top centrifuge tube and spun at 300×*g* (*rcf*) for 1 min. The tip-bound EVs were then washed with 200 μL of PBS (300×*g*, 1 min), and the matrix proteins eluted using 200 μL of 25% glycerol with 1 M ammonium sulfate in PBS (300×*g*, 1 min).

Table 1
Scientific name, reported size, and isolation method used for the extraction of plant-derived EVs. Sample categories: leafy greens (represented in green), vegetables (represented in red), and fruit (represented in blue).

Common Name	Species Name	Size (nm)	Isolation Method	References
Baby Spinach	*Spinacia oleracea*	-	-	-
Lettuce	*Lactuca sativa*	-	-	-
Green Onions	*Allium fistulosum*	-	-	-
Cilantro	*Coriandrum sativum*	-	-	-
Carrots	*Daucus carota subsp. sativus*	150 nm (Average)	Size-Exclusion Chromatography	[65]
Roma Tomato	*Solanum lycopersicum 'Roma'*	-	-	-
Beefsteak Tomato	*Solanum lycopersicum 'Beefsteak'*	100 – 1000 nm	Ultracentrifugation, Density Gradient Centrifugation, and Filtration	[42, 66, 67]
Cucumber	*Cucumis sativus*	-	-	-
Sweet Onion	*Allium cepa 'White onion'*	113 – 153 nm	Ultracentrifugation	[68]
Red Onion	*Allium cepa 'Red onion'*	113– 153 nm	Ultracentrifugation	[68]
Ginger	*Zingiber officinale*	50-800 nm (Average 189 nm)	Ultracentrifugation	[42, 69, 70]
Blueberries	*Vaccinium sect. Cyanococcus*	100 – 800 nm	Ultracentrifugation, Differential Centrifugation	[42, 71]
Cherries	*Prunus avium*	-	-	-
Red Apple	*Malus domestica 'Red Delicious'*	-	-	-
Green Apple	*Malus domestica 'Granny Smith'*	-	-	-
Strawberries	*Fragaria × ananassa*	30 – 191 nm	Ultracentrifugation	[72]
Lime	*Citrus × aurantiifolia*	-	-	-
Lemon Juice	*Citrus limon L.*	50 – 100 nm	Differential Centrifugation, Filtration, Ultracentrifugation	[66]
Orange	*Citrus sinensis*	100 – 800 nm	Differential Centrifugation	[42]
Aloe Vera Juice	*Aloe vera barbadensis*	50 – 200 nm	Ultracentrifugation, Ultrafiltration, Tangential Flow Fractionation	[73]

Finally, the PDEVs were eluted from the C-CP tip surface using 50 μL of 50% glycerol in PBS (300×*g*, 1 min) into an Eppendorf tube conical insert.

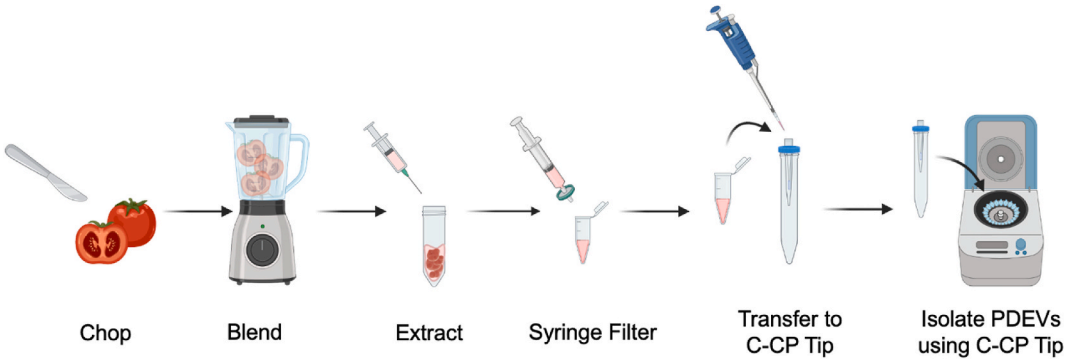

Fig. 1. Diagrammatic representation of the sample processing workflow for the isolation of plant-derived extracellular vesicles (PDEVs) using the capillary-channeled polymer (C-CP) fiber solid-phase extraction tip and a tabletop centrifuge.

2.5. Absorbance/scattering detection

One of the largest sources of imprecision and inaccuracy in EV characterization has been the use of nanoparticle tracking analysis (NTA) as a means of quantifying and sizing of isolates [58,59]. As previous reports from this laboratory have demonstrated, optical absorbance (technically, scattering) measurements are a valid means of EV quantification based on the generation of standard response (calibration) curves using commercial exosome standard stocks or via the method of standard addition [51,54]. The two approaches have been compared in detail in previous works for the quantification of EVs in human biofluids [54]. In this case, the method of standard addition was applied because of the potential for matrix effects across the diverse plant specimens, which could cause the absorbance quantification of EVs to be skewed. Across the previous work with biofluids, the method was able to overcome the intense sample matrix effects, and the absorbance quantification of the EVs using the standard addition method was also able to determine EV concentrations with high precision (<5% RSD) [54]. As done previously, serial additions of the commercially-obtained exosome standard stock were used to create a standard addition response curve. In these experiments, the absorbance of each sample was measured at 203 nm (n = 5) using the NanoVue spectrophotometer. The resulting linear regression was used to determine the concentration of the recovered PDEVs.

Several recent works have employed multiangle light scattering (MALS) detection for human EV size determinations [60–62]. Here, the diameters (actually the root-mean-square (RMS) radii) of the PDEVs of the recovered particles were determined using the DAWN multi-angle light scattering (MALS) detector (Wyatt Technology, Goleta, CA, USA), controlled using the ASTRA software. After the C-CP tip isolation process, the recovered EVs were passed through to the MALS detector cell using a Dionex (Thermo Fisher Scientific, Sunnyvale, CA, USA) Ultimate 3000 HPLC system (LPG-3400SD quaternary pump with MWD-3000 UV–Vis absorbance detector), which was controlled by the Chromeleon 7 software. The experimentally-determined RMS radii were multiplied by 2 to represent the approximate diameter/size of the PDEVs. For the entirety of MALS analyses, the refractive index was set to that of 50% glycerol in PBS, 1.4096 (experimentally determined using a Reichert AR7 Series Automatic Refractometer at 22 °C). Three replicate measurements were collected for each sample in 60-s increments.

2.6. Transmission electron microscopy (TEM)

The biophysical characteristics of the collected PDEVs, including size and shape, were evaluated using a Hitachi HR7830 TEM [56]. The TEM sample preparation was performed as previously reported. Briefly, 7 μL of each EV sample was applied to a copper/formvar grid and incubated at room temperature for 20 min before the excess sample liquid was removed. Next, the EVs were fixed on the grids using 2% paraformaldehyde (RT, 5 min). Afterward, the excess paraformaldehyde was removed from the grids, and they were washed with 50 μL droplets of water for 5 min. The grid was then negatively stained using 50 μL of a filtered 1% uranyl acetate solution (RT, 1 min). After staining, the excess uranyl acetate solution was removed using a paper towel, and the prepared grid was again washed with water before being allowed to dry in a desiccator for 30 min. The size of the vesicles visualized in the TEM micrographs was determined using ImageJ.

2.7. Bradford assay

As stated previously, the removal of matrix proteins is perhaps the most significant challenge in isolation of EVs, whether for fundamental studies or in vector applications. The Bradford assay is the classic means of determining free protein content in diverse media and was used here to assess the presence of free proteins in the plant sample stocks and the removal of those ‘contaminants’ from the test solution following isolation of the PDEVs using the C-CP tips. For this, 250 μL of Bradford reagent was added to 25 μL of each sample stock or the PDEV recovery in a 96 well plate before incubation at room temperature for 20 min and absorbance detection of the Bradford reagent at 595 nm using the Synergy H1 Plate Reader. A standard curve using serial dilutions of a BSA solution was used to determine the total protein concentration of the samples. All samples and standards were applied to the well plate in triplicate.

2.8. Enzyme-linked immunosorbent assay (ELISA)

Analogous to the identification of mammalian EVs based on the presence of the tetraspanin proteins (e.g., CD81), the PEN1 protein serves as a surface marker for PDEVs, while not being present in bacteria-originating EVs. A polyclonal antibody to the PEN1 protein (custom-prepared by CUSABIO, Houston, TX) was employed in an indirect ELISA assay to confirm both the presence and bioactivity of PDEVs after isolation using the C-CP tip method. Prior, the tip-isolated PDEVs were applied to a 100 kDa filter unit, and the latent glycerol was removed, as glycerol is known to interfere with antibody binding [63,64]. The ELISA protocol was performed as previously described [53,54], with samples applied in triplicate. The PEN1 purified protein, obtained from the manufacturer, was used as the positive control, and the neat EV elution buffer – 50% glycerol in PBS was used as the negative control. The Synergy H1 microplate reader was used to detect the chemiluminescent response of the HRP-catalyzed oxidation of the detection substrate.

3. Results and discussion

In a recent review by Innes and colleagues, it was recommended that PDEV researchers pay close attention to progress in methods across all of

EV isolation methodologies, being mindful of the "pitfalls" and challenges commonly experienced during EV research [18]. For example, standardization of relevant isolation and characterization protocols for EVs and PDEVs is largely lacking. Because EVs are not able to be well isolated/characterized, they are not able to be well-classified, causing there to be a lack of field-wide agreement on standard protocols, fundamental structure-function correlations, and EV nomenclature [29]. These disagreements have been limiting in the mammalian EV field as a whole, but particularly in the development of exosome/EV standardized reference materials. With all of these concerns being relevant to PDEV research as well, it is essential for researchers in the PDEV realm to consider these as the field continues to progress. Though all of these shortcomings limit the pursuit of novel PDEV therapeutic approaches, the lack of isolation methods to efficiently provide representative populations of PDEVs is potentially most limiting to the progression of research [18]. In order to evade the limitations of the currently available isolation methods, the hydrophobicity-based solid-phase extraction of PDEVs using C-CP fiber tips has been developed, where fundamental PDEV qualities such as size, integrity, and yield are able to be assessed using downstream characterization techniques.

3.1. Verification of C-CP tip isolated PDEV structure and size by transmission electron microscopy (TEM)

As a complement to other EV characterization methods, TEM is used to confirm the presence of EVs based on the presentation of the characteristic spherical or cup-shaped structure. TEM is used to assess the size, shape, and vesicular integrity of the PDEVs collected using the C-CP fiber tip method. Representative micrographs of a) HEK293 EVs from a commercial standard stock, and b) PDEVs from green onion, c) blueberry, d) ginger, e) strawberry, f) red onion, g) baby spinach, and h) beefsteak tomato samples are shown in Fig. 2. The TEM micrographs confirm the presence of vesicles in the sEV size range (<200 nm) from both the exosome standard stock and the PDEVs isolated from the bulk plant supernatant, all exhibiting the characteristic spherical, membranous shape. Intact exosome-like vesicles are observed, showing the preservation of the membrane integrity after isolation via the C-CP tip method. Of note, there is little evidence of contaminants (debris), despite the complexity of the original sample matrices. Individual vesicles are present in the majority of the samples, but some small vesicle aggregates are observed in the micrographs from the green onion, ginger, and beefsteak tomato samples. Still, the TEM micrographs confirm the presence of 50–200 nm particles with apparent phospholipid bilayer membranes isolated from the plant extracellular fluids using the C-CP fiber spin-down tip.

3.2. Size determination of C-CP tip-isolated EVs using MALS

In addition to TEM sizing of the vesicles, Nanosight nanoparticle tracking analysis (NTA) is commonly used for size determinations of EVs [65,66]. However, many reports reveal concerns with the accuracy of EV size determinations via NTA due to variability/irreproducibility in size determinations and number densities, and because the method is not able to differentiate between EVs and large protein aggregates of EV-like size [67,68]. In order to address these limitations during the PDEV size determinations, the MALS detection method has been previously suggested [60,69,70].

The average sizes of the PDEVs recovered from each plant sample type as determined by MALS are shown in Fig. 3. The C-CP tip-isolated PDEVs yield average diameters of 32–580 nm across the plant sample stocks, with an average diameter of 189 nm across all sample types. These PDEV size determinations align well with the previously-reported diameters as presented in Table 1 for those plant samples subjected to other EV isolation workflows, and with the TEM micrographs shown in Fig. 2, where the exosome/EV-like size and structure of the recovered vesicles are shown. The MALS analysis average diameters of the C-CP tip-eluted PDEVs are also in line with EVs recovered from human biofluids using the C-CP tip isolation method [51,54]. Despite the vast differences in the PDEV sources, the relative precision of the MALS determinations of average PDEV diameters is remarkable versus NTA analysis, with less than 5% RSD across the triplicate size determinations of the PDEVs recovered from each plant source. Though there does seem to be some correlation between the biophysical characteristics of PDEVs obtained from the specific plant sources included here, future works focusing on the comprehensive characterization of the PDEVs from these plant stocks are required before species-specific generalizations regarding PDEV characteristics can be made.

3.3. Quantification of recovered PDEVs via UV–vis absorbance

The quantification of EVs from human biofluid and cell culture sources by optical absorbance at 203 nm has been previously demonstrated [51,54,71], using response curves generated from exosome stock solutions or via the standard addition method. To clarify, the "absorbance" response observed at the 203 nm wavelength is not accredited to electronic transitions of individual analyte molecules. More accurately, the absorbance detection is due to the Mie scattering by the EV nanobodies, which is proportional to the concentration of EVs in solution.

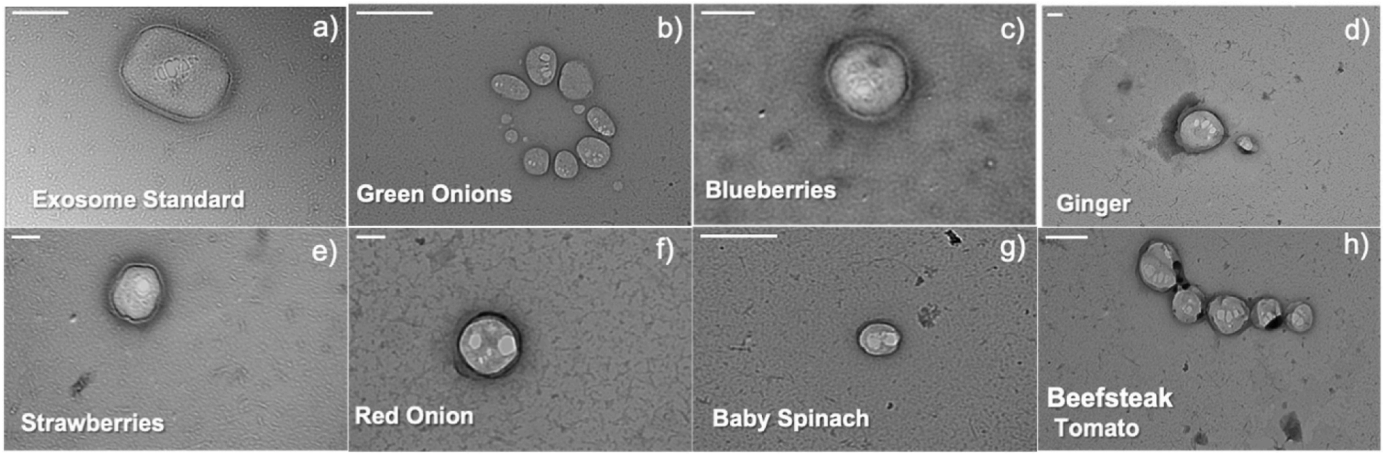

Fig. 2. Transmission electron micrographs of commercial EVs from a) HEK293 exosome standards, and plant-derived extracellular vesicles (PDEVs) from b) green onion, c) blueberry, d) ginger, e) strawberry, f) red onion, g) baby spinach, and h) beefsteak tomato samples following isolation using the C-CP fiber spin-down tip method. The TEM images were taken using the Hitachi HT7830. Scalebar = 100 nm.

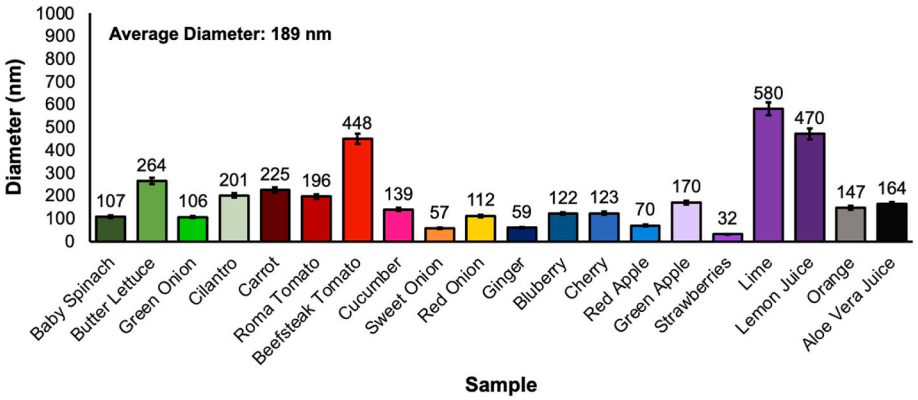

Fig. 3. Size determinations of the C-CP tip isolated PDEVs using the Wyatt Dawn MALS instrument. Presented are the average sizes of the PDEVs resulting from 3 consecutive 60-s runs.

Conveniently, the absorbance spectra obtained for the PDEVs from all sample types follow the EV-characteristic scattering/absorbance responses, where an exponential decrease in absorbance response is observed (200–700 nm, $\lambda_{max} = 203$ nm).

The EV standard addition quantification method is applied here for the quantification of PDEVs recovered from the plant sample extracts after isolation using the C-CP tip method, as shown in Fig. 4. Using this quantitative approach, number densities of 1×10^{10} to 2×10^{11} PDEVs were obtained via processing of only 100 μL of plant sample extracts (Fig. 4a). The largest numbers of PDEVs were obtained from the beefsteak tomato and red onion samples. Since the original mass of the plant samples stocks differed here, a per mass recovery comparison is warranted as a better reflection on the EV-production characteristics of the species. As shown in Fig. 4b, the PDEVs from the butter lettuce and cilantro samples were recovered in higher concentrations with respect to starting material mass, accounting for ~3.6×10^9 EVs per gram of starting material. Alternatively, those PDEVs obtained from the fruit sample category were approximately 4 times lower with respect to

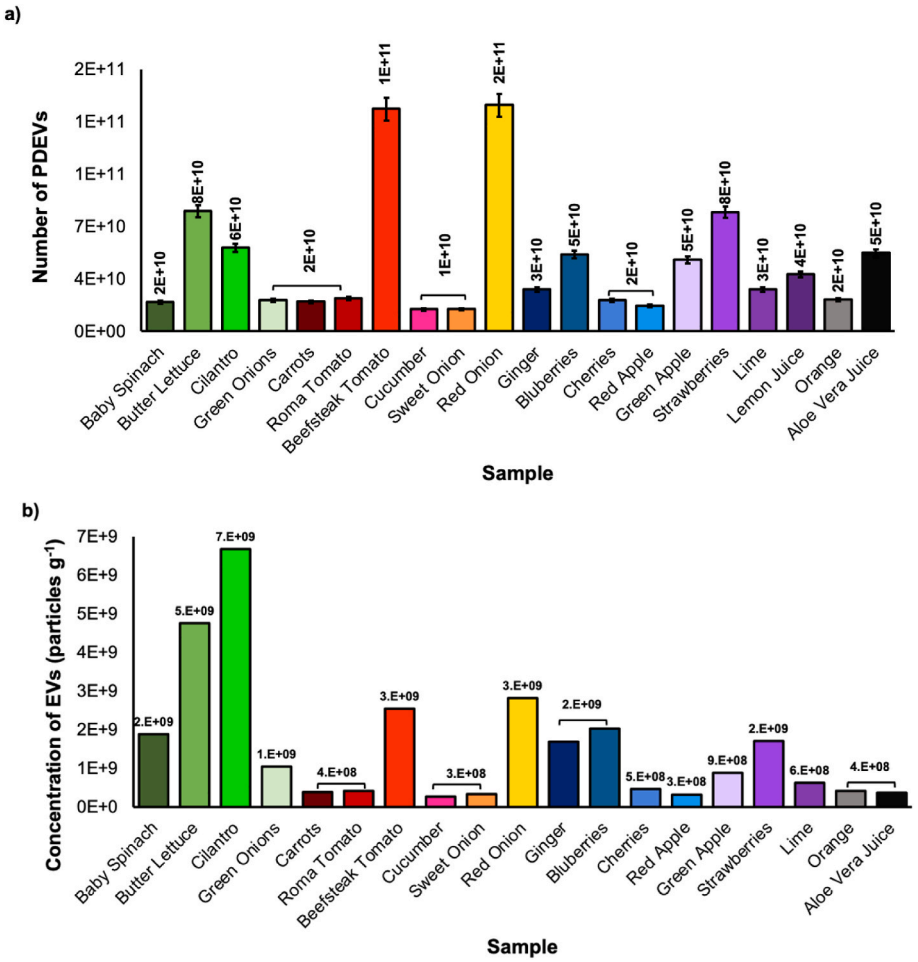

Fig. 4. a) Numbers of recovered PDEVs using the C-CP spin-down tip isolation method, determined using the method of standard addition, and b) recovered PDEV concentrations with respect to the mass of starting material.

starting mass, with 8.4×10^8 EVs per gram of starting material obtained on average. At this point, there is no body of literature suggesting which sorts of species should produce more or less EVs. There are also aspects of growth conditions, stress, etc. which surely will contribute to variation within species. Despite the growing body of PDEV literature, none of the identified previous works have attempted to provide a means of efficient vesicle quantification, as again the methodologies are sorely lacking, as is a well-characterized standardized reference material for PDEVs and EVs in general. At this point, there is no way to verify the accuracy of this quantification effort, but the absorbance quantification-determined values agree with the MALS particle count by plus/minus 10%, based on the flow rate and dilution factor of the PDEVs upon injection into the instrument. Additionally, in the realm of mammalian EV determinations, the C-CP tip isolation coupled with absorbance detection has proven to be a reliable approach [51,55]. Though there is some concern with the mismatch of the EV stock source used in this quantification effort, the method of standard addition employing an alternative EV stock of known concentration (assuming the biophysical characteristics of the stock are similar to that of PDEVs) does allow for the quantification of PDEVs to be reproducibly performed.

3.4. Purity assessment of PDEV isolates via bradford assay

Bradford assays are commonly employed for total protein content determinations in diverse biospecimens and were used here to determine the concentration of protein in the native plant sample extracts, then to quantify the removal of the contaminant protein species by the C-CP tip isolation/purification method. To be clear, there is the expectation that some detectable proteins would be present in the PDEV isolate solutions, as proteins decorating the vesicle shells will register positively via the Bradford assay. Presented in Fig. 5 are the Bradford assay-determined total protein concentrations for each plant sample extract and their respective PDEV isolate solutions. The Roma tomato, red onion, and cherry sample stocks contained the highest starting protein concentrations (>1000 μg mL^{-1}), which intuitively makes sense due to the original masses of these samples ranging from 45 to 60 g of starting material, which is in the upper quartile of mass for the samples employed in this study (average: 35 g, range: 11–60 g). Regardless of the significant differences in original protein content, after processing the plant stocks using the C-CP tip method, the total protein concentrations for each PDEV extract were reduced by 48–95%. All of the recovered PDEV collections resulted in total protein concentrations of less than 100 μg mL^{-1}, which is sufficient given the high concentration of PDEVs recovered in the assessed fraction, and with precise (<6% RSD) determinations of the total protein concentration of the PDEV stocks. The purification of the PDEVs from matrix contaminants based on the decrease in total protein content is also comparable to that obtained from the EVs purified from human biofluids [54]. Again, Bradford assays have not been widely employed for the plant or PDEV stocks, so a point of comparison study comparing the total protein concentration of plant and PDEV stocks is undoubtedly warranted. It is hypothesized that the high purity and high yields using the C-CP tip will translate to broad use of the materials for PDEV isolations in comparison to UC sample processing.

A critical EV purity metric is the concentration of EVs versus the total protein content with respect to volume in the isolate solutions [72,73]. In this regard, an EV-to-protein purity ratio of 3×10^{10} particles μg^{-1} of protein is the metric used to qualify a population of EVs as "pure" [72,74]. In comparing to the absorbance-determined concentrations of the recovered PDEVs to the total protein values from this Bradford assay, all of the PDEV recoveries here are considered to be pure, as shown in Fig. 6. On average, the PDEVs recovered from the leafy green (1.95×10^{11} PDEVs μg^{-1}) sample category were of the highest purity, followed by those from the vegetable (1.87×10^{11} PDEVs μg^{-1}) and fruit (7.05×10^{10} PDEVs μg^{-1}) categories respectively. Importantly, the purity of the PDEVs obtained here are quite comparable to those obtained for human urine samples using an identical C-CP tip isolation protocol [54]. Furthermore, as a point of reference, the EVs obtained using this isolation method have 10 times higher purity than EVs processed using competitive UC and polymeric precipitation EV isolation methods [54]. Future works to directly compare the isolation performance of the C-CP tip to other traditionally-used EV isolation techniques are necessary for the case of PDEVs. Still, the data presented here suggest that the previously demonstrated benefits of high purity and yield through the processing of EV-containing biofluids using C-CP tip methods will translate to PDEVs.

3.5. PEN1 assessment via an indirect enzyme-linked immunosorbent assay (ELISA)

Just as tetraspanin proteins have been used to verify the identity and bioactivity of mammalian EVs [29,75,76], immunoassays to the PEN1 protein have been employed to confirm the presence and activity of PDEVs [17,18,27,77]. While no universally-expressed PDEV marker exists, the PEN1 protein has been identified at significant concentrations in PDEV isolates. As such, PEN1 has been employed as a PDEV marker protein during immunoassays and is also applied for this purpose. It should be reiterated here that positive response to PEN1 does not allow

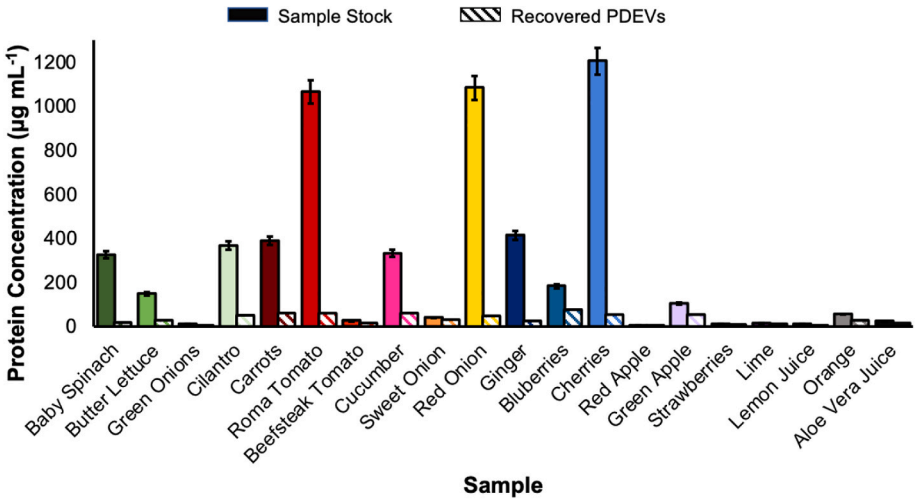

Fig. 5. Total protein content (as determined by Bradford assays) of raw samples and the resulting PDEV isolates using the C-CP spin-down tip isolation method. All samples were analyzed in triplicate, corrected for the average response of triplicate blanks.

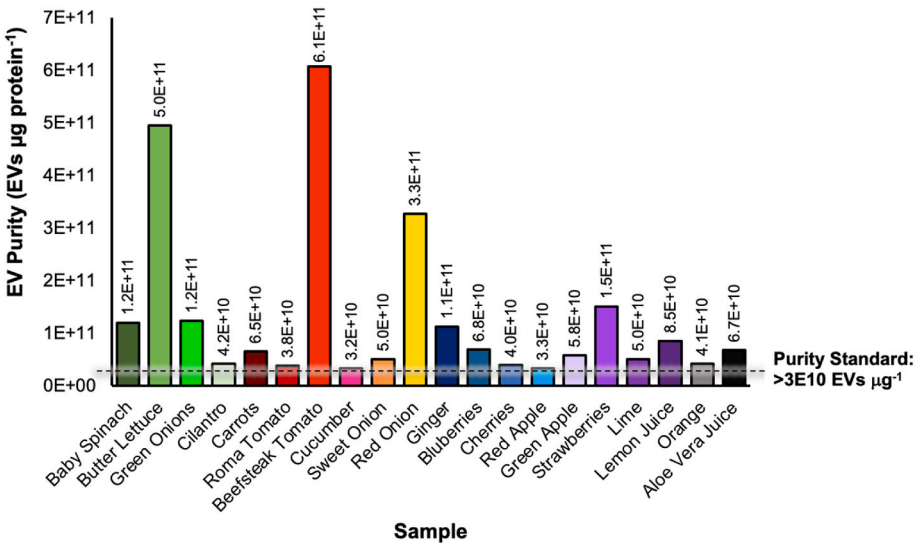

Fig. 6. Determined PDEV purities based on the EV recoveries presented in Fig. 4, and the residual protein content presented in Fig. 5.

for differentiation between those EVs that existed in the intra- or extracellular regions of the original plant samples, but there will be no response for those EVs which are bacterial in nature.

As shown in Fig. 7, each of the PDEV isolates yields a positive response in the PEN1 ELISA. Serial dilutions of the PEN1 purified protein were used to create a standard curve of linear response ($R^2 = 0.995$) for ELISA quantification purposes, and the concentration of PEN1 in each sample's PDEV recovery was determined. With this, the presence of the PEN1 protein in the eluates is semi-quantitatively assessed. As shown, 315–1,079 ng of PEN1 were detected in the PDEV eluates, with the highest response for the PEN1 seen in the red apple recovery. It must be emphasized, that the preponderance of expression of PEN1 in each of these plant species has not been thoroughly explored. Indeed, just as in the case of different mammalian cells from the same species, which display highly variable levels of the respective tetraspanins, it would not be expected that PEN1 would be expressed to the same extents in these species. However, with the assumption that contaminant-sourced EVs (i.e. bacterial OMVs) should not express the PDEV-specific PEN1 protein, Fig. 7 provides evidence to suggest that the recovered vesicles are of plant origin.

4. Conclusions

While the evolution of methodologies for the isolation of EVs from mammalian sources is very much in a mode of expansion, methodologies applicable to plant-derived EVs are very much in their infancy. The C-CP fiber spin down tip method has been demonstrated as an efficient, practical method for the isolation of PDEVs from 20 plant sample sources, including those from vegetable, fruit, and leafy green sample categories. It is important to note that the present authors have not yet identified works describing the isolation of exosome-like vesicles in baby spinach, butter lettuce, green onion, cilantro, Roma tomato, cucumber, cherry, apple (green and red), and lime samples. Because of this, the presented work is potentially the first application of PDEV isolations from these plant types. The C-CP spin-down tip method yields representative collections of PDEVs, with significant benefits relative to standard methods based on centrifugation or size exclusion isolation. The HIC-based C-CP fiber spin down tip method is demonstrated to provide the sample integrity, yield, and purity required to allow for critical PDEV characterization studies to be performed. High purity recoveries are achieved in less than 15 min processing times, using sample extract volumes of only 100 µL. The materials costs for each isolation are <$1 and are affected on simple benchtop centrifuges.

While much promise is demonstrated here, challenges remain in terms of implemented methods of extraction which ensure that the isolated vesicles are truly extracellular in nature [18]. The use of mechanical homogenization certainly has the potential to disrupt the cellular structure of plant materials and so means of assuring proper sampling are required as discussed by Innes and co-workers [27,45]. Additionally, methods of sample preparation which alleviate potential

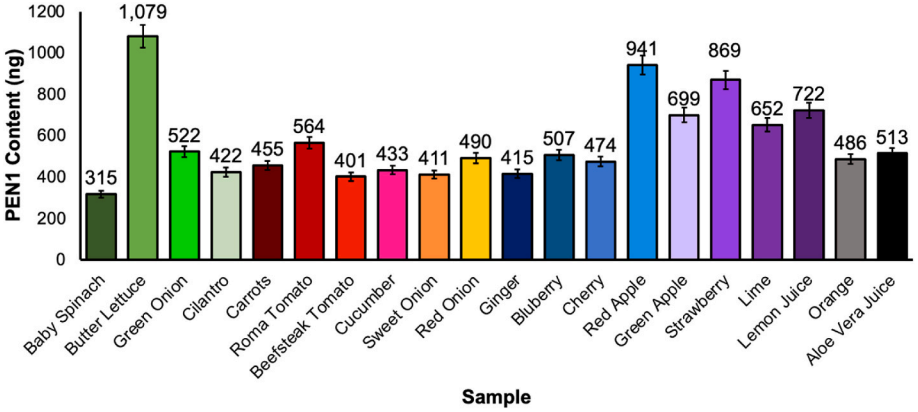

Fig. 7. Indirect ELISA confirmation of the presence of the PEN1 marker protein for PDEVs recovered from plant samples using the C-CP spin-down tip method. Samples were analyzed in triplicate, corrected for the average response of triplicate blanks.

contamination from bacterially-generated EVs must be part of the overall processing protocol. Further, it is indeed possible that in the TEM imaging, MALS analysis, and absorbance-based quantification of the PDEV recoveries, there is the potential that EVs from bacterial contaminant sources would behave similarly. Future works are necessary to definitively associate the C-CP tip recovered vesicles with their true plant origins and assess the extent of co-isolation of these contaminant species.

This innovative approach to PDEV isolations will enable more comprehensive assessments of both fundamental and therapeutic relevance to be performed with higher efficiency and using a practical workflow. As in the case of mammalian EV populations, use of mass spectrometric proteomics between the species is a natural avenue of pursuit. It is anticipated that future developments of the isolation method presented during this work can be scaled-up towards volume and concentration levels of relevance towards the production of PDEV therapeutic vectors.

Credit author statement

Kaylan K. Jackson: Methodology, Data curation, Visualization, Writing – original draft; **Carolina Mata**: Methodology; **R. Kenneth Marcus**: Conceptualization, Supervision, Writing – Reviewing and Editing

Declaration of competing interest

The authors declare that they have no known competing financial interests or personal relationships that could have appeared to influence the work reported in this paper.

Data availability

Data will be made available on request.

Acknowledgements

Financial support from the National Science Foundation under grant no. CHE-2107882 is gratefully acknowledged. Helpful conversations with Prof. Roger Innes (Indiana University, USA) in the initial stages of this project are acknowledged.

References

[1] S. Gill, R. Catchpole, P. Forterre, Extracellular membrane vesicles in the three domains of life and beyond, FEMS Microbiol. Rev. 43 (3) (2019) 273–303.
[2] E. Woith, G. Fuhrmann, M.F. Melzig, Extracellular vesicles-connecting kingdoms, Int. J. Mol. Sci. 20 (22) (2019) 5695.
[3] E.I. Buzas, B. Gyorgy, G. Nagy, A. Falus, S. Gay, Emerging role of extracellular vesicles in inflammatory diseases, Nat. Rev. Rheumatol. 10 (6) (2014) 356–364.
[4] C.M. Boulanger, X. Loyer, P.E. Rautou, N. Amabile, Extracellular vesicles in coronary artery disease, Nat. Rev. Cardiol. 14 (5) (2017) 259–272.
[5] A.G. Thompson, E. Gray, S.M. Heman-Ackah, I. Mager, K. Talbot, S.E. Andaloussi, M.J. Wood, M.R. Turner, Extracellular vesicles in neurodegenerative disease - pathogenesis to biomarkers, Nat. Rev. Neurol. 12 (6) (2016) 346–357.
[6] Y. Zhang, Y. Liu, H. Liu, W.H. Tang, Exosomes: biogenesis, biologic function and clinical potential, Cell Biosci. 9 (1) (2019) 19.
[7] I.L. Colao, R. Corteling, D. Bracewell, I. Wall, Manufacturing exosomes: a promising therapeutic platform, Trends Mol. Med. 24 (3) (2018) 242–256.
[8] T. Yamashita, Y. Takahashi, Y. Takakura, Possibility of exosome-based therapeutics and challenges in production of exosomes eligible for therapeutic application, Biol. Pharm. Bull. 41 (6) (2018) 835–842.
[9] A.T. Jan, Outer membrane vesicles (OMVs) of gram-negative bacteria: a perspective update, Front. Microbiol. 8 (2017) 1053.
[10] A. Kulp, M.J. Kuehn, Biological functions and biogenesis of secreted bacterial outer membrane vesicles, Annu. Rev. Microbiol. 64 (1) (2010) 163–184.
[11] M. Samuel, M. Bleackley, M. Anderson, S. Mathivanan, Extracellular vesicles including exosomes in cross kingdom regulation: a viewpoint from plant-fungal interactions, Front. Plant Sci. 6 (2015) 766.
[12] J.S. Schorey, Y. Cheng, P.P. Singh, V.L. Smith, Exosomes and other extracellular vesicles in host-pathogen interactions, EMBO Rep. 16 (1) (2015) 24–43.
[13] G. Coakley, R.M. Maizels, A.H. Buck, Exosomes and other extracellular vesicles: the new communicators in parasite infections, Trends Parasitol. 31 (10) (2015) 477–489.
[14] Q. An, A.J. van Bel, R. Huckelhoven, Do plant cells secrete exosomes derived from multivesicular bodies? Plant Signal. Behav. 2 (1) (2007) 4–7.
[15] P. Baldrich, B.D. Rutter, H.Z. Karimi, R. Podicheti, B.C. Meyers, R.W. Innes, Plant extracellular vesicles contain diverse small RNA species and are enriched in 10- to 17-nucleotide "tiny" RNAs, Plant Cell 31 (2) (2019) 315–324.
[16] M. Pinedo, L. de la Canal, C. de Marcos Lousa, A call for Rigor and standardization in plant extracellular vesicle research, J. Extracell. Vesicles 10 (6) (2021), e12048.
[17] B.D. Rutter, R.W. Innes, Extracellular vesicles as key mediators of plant-microbe interactions, Curr. Opin. Plant Biol. 44 (2018) 16–22.
[18] B.D. Rutter, R.W. Innes, Growing pains: addressing the pitfalls of plant extracellular vesicle research, New Phytol. 228 (5) (2020) 1505–1510.
[19] N. Kameli, A. Dragojlovic-Kerkache, P. Savelkoul, F.R. Stassen, Plant-derived extracellular vesicles: current findings, challenges, and future applications, Membranes 11 (6) (2021) 411.
[20] M.S. Manocha, M. Shaw, Occurrence of lomasomes in mesophyll cells of 'khapli' wheat, Nature 203 (4952) (1964) 1402–1403.
[21] W. Halperin, W.A. Jensen, Ultrastructural changes during growth and embryogenesis in carrot cell cultures, J Ultrastruct Res 18 (3) (1967) 428–443.
[22] T. Karamanidou, A. Tsouknidas, Plant-derived extracellular vesicles as therapeutic nanocarriers, Int. J. Mol. Sci. 23 (1) (2022) 191.
[23] J. Mu, X. Zhuang, Q. Wang, H. Jiang, Z.B. Deng, B. Wang, L. Zhang, S. Kakar, Y. Jun, D. Miller, H.G. Zhang, Interspecies communication between plant and mouse gut host cells through edible plant derived exosome-like nanoparticles, Mol. Nutr. Food Res. 58 (7) (2014) 1561–1573.
[24] Q. An, R. Huckelhoven, K.H. Kogel, A.J. van Bel, Multivesicular bodies participate in a cell wall-associated defence response in barley leaves attacked by the pathogenic powdery mildew fungus, Cell Microbiol. 8 (6) (2006) 1009–1019.
[25] O.N. Johansson, E. Fantozzi, P. Fahlberg, A.K. Nilsson, N. Buhot, M. Tor, M. X. Andersson, Role of the penetration-resistance genes PEN1, PEN2 and PEN3 in the hypersensitive response and race-specific resistance in Arabidopsis thaliana, Plant J. 79 (3) (2014) 466–476.
[26] G. Liu, G. Kang, S. Wang, Y. Huang, Q. Cai, Extracellular vesicles: emerging players in plant defense against pathogens, Front. Plant Sci. 12 (2021), 757925.
[27] B.D. Rutter, R.W. Innes, Extracellular vesicles isolated from the leaf apoplast carry stress-response proteins, Plant Physiol 173 (1) (2017) 728–741.
[28] J. Zhang, Y. Qiu, K. Xu, Characterization of GFP-AtPEN1 as a marker protein for extracellular vesicles isolated from Nicotiana benthamiana leaves, Plant Signal. Behav. 15 (9) (2020), 1791519.
[29] C. Thery, K.W. Witwer, E. Aikawa, M.J. Alcaraz, J.D. Anderson, R. Andriantsitohaina, A. Antoniou, T. Arab, F. Archer, G.K. Atkin-Smith, D.C. Ayre, J.M. Bach, D. Bachurski, H. Baharvand, L. Balaj, S. Baldacchino, N.N. Bauer, A. A. Baxter, M. Bebawy, C. Beckham, A. Bedina Zavec, A. Benmoussa, A.C. Berardi, P. Bergese, E. Bielska, C. Blenkiron, S. Bobis-Wozowicz, E. Boilard, W. Boireau, A. Bongiovanni, F.E. Borras, S. Bosch, C.M. Boulanger, X. Breakefield, A.M. Breglio, M.A. Brennan, D.R. Brigstock, A. Brisson, M.L. Broekman, J.F. Bromberg, P. Bryl-Gorecka, S. Buch, A.H. Buck, D. Burger, S. Busatto, D. Buschmann, B. Bussolati, E. I. Buzas, J.B. Byrd, G. Camussi, D.R. Carter, S. Caruso, L.W. Chamley, Y.T. Chang, C. Chen, S. Chen, L. Cheng, A.R. Chin, A. Clayton, S.P. Clerici, A. Cocks, E. Cocucci, R.J. Coffey, A. Cordeiro-da-Silva, Y. Couch, F.A. Coumans, B. Coyle, R. Crescitelli, M.F. Criado, C. D'Souza-Schorey, S. Das, A. Datta Chaudhuri, P. de Candia, E.F. De Santana, O. De Wever, H.A. Del Portillo, T. Demaret, S. Deville, A. Devitt, B. Dhondt, D. Di Vizio, L.C. Dieterich, V. Dolo, A.P. Dominguez Rubio, M. Dominici, M.R. Dourado, T.A. Driedonks, F.V. Duarte, H.M. Duncan, R. M. Eichenberger, K. Ekstrom, S. El Andaloussi, C. Elie-Caille, U. Erdbrugger, J. M. Falcon-Perez, F. Fatima, J.E. Fish, M. Flores-Bellver, A. Forsonits, A. Frelet-Barrand, F. Fricke, G. Fuhrmann, S. Gabrielsson, A. Gamez-Valero, C. Gardiner, K. Gartner, R. Gaudin, Y.S. Gho, B. Giebel, C. Gilbert, M. Gimona, I. Giusti, D. C. Goberdhan, A. Gorgens, S.M. Gorski, D.W. Greening, J.C. Gross, A. Gualerzi, G. N. Gupta, D. Gustafson, A. Handberg, R.A. Haraszti, P. Harrison, H. Hegyesi, A. Hendrix, A.F. Hill, F.H. Hochberg, K.F. Hoffmann, B. Holder, H. Holthofer, B. Hosseinkhani, G. Hu, Y. Huang, V. Huber, S. Hunt, A.G. Ibrahim, T. Ikezu, J. M. Inal, M. Isin, A. Ivanova, H.K. Jackson, S. Jacobsen, S.M. Jay, M. Jayachandran, G. Jenster, L. Jiang, S.M. Johnson, J.C. Jones, A. Jong, T. Jovanovic-Talisman, S. Jung, R. Kalluri, S.I. Kano, S. Kaur, Y. Kawamura, E.T. Keller, D. Khamari, E. Khomyakova, A. Khvorova, P. Kierulf, K.P. Kim, T. Kislinger, M. Klingeborn, D. J. Klinke 2nd, M. Kornek, M.M. Kosanovic, A.F. Kovacs, E.M. Kramer-Albers, S. Krasemann, M. Krause, I.V. Kurochkin, G.D. Kusuma, S. Kuypers, S. Laitinen, S. M. Langevin, L.R. Languino, J. Lannigan, C. Lasser, L.C. Laurent, G. Lavieu, E. Lazaro-Ibanez, S. Le Lay, M.S. Lee, Y.X.F. Lee, D.S. Lemos, M. Lenassi, A. Leszczynska, I.T. Li, K. Liao, S.F. Libregts, E. Ligeti, R. Lim, S.K. Lim, A. Line, K. Linnemannstons, A. Llorente, C.A. Lombard, M.J. Lorenowicz, A.M. Lorincz, J. Lotvall, J. Lovett, M.C. Lowry, X. Loyer, Q. Lu, B. Lukomska, T.R. Lunavat, S. L. Maas, H. Malhi, A. Marcilla, J. Mariani, J. Mariscal, E.S. Martens-Uzunova, L. Martin-Jaular, M.C. Martinez, V.R. Martins, M. Mathieu, S. Mathivanan, M. Maugeri, L.K. McGinnis, M.J. McVey, D.G. Meckes Jr., K.L. Meehan, I. Mertens, V.R. Minciacchi, A. Moller, M. Moller Jorgensen, A. Morales-Kastresana, J. Morhayim, F. Mullier, M. Muraca, L. Musante, V. Mussack, D.C. Muth, K. H. Myburgh, T. Najrana, M. Nawaz, I. Nazarenko, P. Nejsum, C. Neri, T. Neri, R. Nieuwland, L. Nimrichter, J.P. Nolan, E.N. Nolte-'t Hoen, N. Noren Hooten, L. O'Driscoll, T. O'Grady, A. O'Loghlen, T. Ochiya, M. Olivier, A. Ortiz, L.A. Ortiz, X. Osteikoetxea, O. Ostergaard, M. Ostrowski, J. Park, D.M. Pegtel, H. Peinado, F. Perut, M.W. Pfaffl, D.G. Phinney, B.C. Pieters, R.C. Pink, D.S. Pisetsky, E. Pogge von Strandmann, I. Polakovicova, I.K. Poon, B.H. Powell, I. Prada, L. Pulliam,

P. Quesenberry, A. Radeghieri, R.L. Raffai, S. Raimondo, J. Rak, M.I. Ramirez, G. Raposo, M.S. Rayyan, N. Regev-Rudzki, F.L. Ricklefs, P.D. Robbins, D. D. Roberts, S.C. Rodrigues, E. Rohde, S. Rome, K.M. Rouschop, A. Rughetti, A. E. Russell, P. Saa, S. Sahoo, E. Salas-Huenuleo, C. Sanchez, J.A. Saugstad, M. J. Saul, R.M. Schiffelers, R. Schneider, T.H. Schoyen, A. Scott, E. Shahaj, S. Sharma, O. Shatnyeva, F. Shekari, G.V. Shelke, A.K. Shetty, K. Shiba, P.R. Siljander, A. M. Silva, A. Skowronek, O.L. Snyder 2nd, R.P. Soares, B.W. Sodar, C. Soekmadji, J. Sotillo, P.D. Stahl, W. Stoorvogel, S.L. Stott, E.F. Strasser, S. Swift, H. Tahara, M. Tewari, K. Timms, S. Tiwari, R. Tixeira, M. Tkach, W.S. Toh, R. Tomasini, A. C. Torrecilhas, J.P. Tosar, V. Toxavidis, L. Urbanelli, P. Vader, B.W. van Balkom, S. G. van der Grein, J. Van Deun, M.J. van Herwijnen, K. Van Keuren-Jensen, G. van Niel, M.E. van Royen, A.J. van Wijnen, M.H. Vasconcelos, I.J. Vechetti Jr., T. D. Veit, L.J. Vella, E. Velot, F.J. Verweij, B. Vestad, J.L. Vinas, T. Visnovitz, K. V. Vukman, J. Wahlgren, D.C. Watson, M.H. Wauben, A. Weaver, J.P. Webber, V. Weber, A.M. Wehman, D.J. Weiss, J.A. Welsh, S. Wendt, A.M. Wheelock, Z. Wiener, L. Witte, J. Wolfram, A. Xagorari, P. Xander, J. Xu, X. Yan, M. Yanez-Mo, H. Yin, Y. Yuana, V. Zappulli, J. Zarubova, V. Zekas, J.Y. Zhang, Z. Zhao, L. Zheng, A.R. Zheutlin, A.M. Zickler, P. Zimmermann, A.M. Zivkovic, D. Zocco, E. K. Zuba-Surma, Minimal information for studies of extracellular vesicles 2018 (MISEV2018): a position statement of the International Society for Extracellular Vesicles and update of the MISEV2014 guidelines, J. Extracell. Vesicles 7 (1) (2018), 1535750.

[30] S. Raimondo, F. Naselli, S. Fontana, F. Monteleone, A. Lo Dico, L. Saieva, G. Zito, A. Flugy, M. Manno, M.A. Di Bella, G. De Leo, R. Alessandro, Citrus limon-derived nanovesicles inhibit cancer cell proliferation and suppress CML xenograft growth by inducing TRAIL-mediated cell death, Oncotarget 6 (23) (2015) 19514–19527.

[31] G. Pocsfalvi, L. Turiak, A. Ambrosone, P. Del Gaudio, G. Puska, I. Fiume, T. Silvestre, K. Vekey, Protein biocargo of citrus fruit-derived vesicles reveals heterogeneous transport and extracellular vesicle populations, J. Plant Physiol. 229 (2018) 111–121.

[32] J. Xiao, S. Feng, X. Wang, K. Long, Y. Luo, Y. Wang, J. Ma, Q. Tang, L. Jin, X. Li, M. Li, Identification of exosome-like nanoparticle-derived microRNAs from 11 edible fruits and vegetables, PeerJ 6 (2018), e5186.

[33] X. Zhuang, Z.B. Deng, J. Mu, L. Zhang, J. Yan, D. Miller, W. Feng, C.J. McClain, H. G. Zhang, Ginger-derived nanoparticles protect against alcohol-induced liver damage, J. Extracell. Vesicles 4 (1) (2015), 28713.

[34] Y. Teng, Y. Ren, M. Sayed, X. Hu, C. Lei, A. Kumar, E. Hutchins, J. Mu, Z. Deng, C. Luo, K. Sundaram, M.K. Sriwastva, L. Zhang, M. Hsieh, R. Reiman, B. Haribabu, J. Yan, V.R. Jala, D.M. Miller, K. Van Keuren-Jensen, M.L. Merchant, C.J. McClain, J.W. Park, N.K. Egilmez, H.G. Zhang, Plant-derived exosomal MicroRNAs shape the gut microbiota, Cell Host Microbe 24 (5) (2018) 637–652 e8.

[35] M. Potesta, A. Minutolo, A. Gismondi, L. Canuti, M. Kenzo, V. Roglia, F. Macchi, S. Grelli, A. Canini, V. Colizzi, C. Montesano, Cytotoxic and apoptotic effects of different extracts of Moringa oleifera Lam on lymphoid and monocytoid cells, Exp. Ther. Med. 18 (1) (2019) 5–17.

[36] M. Potesta, V. Roglia, M. Fanelli, E. Pietrobono, A. Gismondi, S. Vumbaca, R. G. Nguedia Tsangueu, A. Canini, V. Colizzi, S. Grelli, A. Minutolo, C. Montesano, Effect of microvesicles from Moringa oleifera containing miRNA on proliferation and apoptosis in tumor cell lines, Cell Death Dis. 6 (1) (2020) 43.

[37] E. Woith, M.F. Melzig, Extracellular vesicles from fresh and dried plants—simultaneous purification and visualization using gel electrophoresis, Int. J. Mol. Sci. 20 (2) (2019) 357.

[38] P. Li, M. Kaslan, S.H. Lee, J. Yao, Z. Gao, Progress in Exosome Isolation Techniques, Theranostics 7 (3) (2017) 789–804.

[39] G.K. Patel, M.A. Khan, H. Zubair, S.K. Srivastava, M. Khushman, S. Singh, A. P. Singh, Comparative analysis of exosome isolation methods using culture supernatant for optimum yield, purity and downstream applications, Sci. Rep. 9 (1) (2019) 5335.

[40] N. Ludwig, T.L. Whiteside, T.E. Reichert, Challenges in exosome isolation and analysis in health and disease, Int. J. Mol. Sci. 20 (19) (2019) 4684.

[41] J.B. Burton, N.J. Carruthers, P.M. Stemmer, Enriching Extracellular Vesicles for Mass Spectrometry, Mass Spectrom Rev, 2021 n/a(n/a).

[42] I. Jalaludin, D.M. Lubman, J. Kim, A Guide to Mass Spectrometric Analysis of Extracellular Vesicle Proteins for Biomarker Discovery, Mass Spectrom Rev, 2021, e21749 n/a(n/a).

[43] Y. Cui, J. Gao, Y. He, L. Jiang, Plant extracellular vesicles, Protoplasma 257 (1) (2020) 3–12.

[44] H. Zand Karimi, P. Baldrich, B.D. Rutter, L. Borniego, K.K. Zajt, B.C. Meyers, R. W. Innes, Arabidopsis apoplastic fluid contains sRNA- and circular RNA-protein complexes that are located outside extracellular vesicles, Plant Cell 34 (5) (2022) 1863–1881.

[45] B.D. Rutter, K.L. Rutter, R.W. Innes, Isolation and quantification of plant extracellular vesicles, Bio Protoc 7 (17) (2017), e2533.

[46] P. Gourabathini, M.T. Brandl, K.S. Redding, J.H. Gunderson, S.G. Berk, Interactions between food-borne pathogens and protozoa isolated from lettuce and spinach, Appl. Environ. Microbiol. 74 (8) (2008) 2518–2525.

[47] R. Acevedo, S. Fernandez, C. Zayas, A. Acosta, M.E. Sarmiento, V.A. Ferro, E. Rosenqvist, C. Campa, D. Cardoso, L. Garcia, J.L. Perez, Bacterial outer membrane vesicles and vaccine applications, Front. Immunol. 5 (2014) 121.

[48] T.F. Bruce, T.J. Slonecki, L. Wang, S. Huang, R.R. Powell, R.K. Marcus, Exosome isolation and purification via hydrophobic interaction chromatography using a polyester, capillary-channeled polymer fiber phase, Electrophoresis 40 (4) (2019) 571–581.

[49] S. Huang, L. Wang, T.F. Bruce, R.K. Marcus, Isolation and quantification of human urinary exosomes by hydrophobic interaction chromatography on a polyester capillary-channeled polymer fiber stationary phase, Anal. Bioanal. Chem. 411 (25) (2019) 6591–6601.

[50] S. Huang, L. Wang, T.F. Bruce, R.K. Marcus, Evaluation of exosome loading characteristics in their purification via a glycerol-assisted hydrophobic interaction chromatography method on a polyester, capillary-channeled polymer fiber phase, Biotechnol. Prog. 36 (5) (2020) e2998.

[51] K.K. Jackson, R.R. Powell, T.F. Bruce, R.K. Marcus, Solid-phase extraction of exosomes from diverse matrices via a polyester capillary-channeled polymer (C-CP) fiber stationary phase in a spin-down tip format, Anal. Bioanal. Chem. 412 (19) (2020) 4713–4724.

[52] L. Wang, T.F. Bruce, S. Huang, R.K. Marcus, Isolation and quantitation of exosomes isolated from human plasma via hydrophobic interaction chromatography using a polyester, capillary-channeled polymer fiber phase, Anal. Chim. Acta 1082 (2019) 186–193.

[53] S. Huang, X. Ji, K.K. Jackson, D.M. Lubman, M.B. Ard, T.F. Bruce, R.K. Marcus, Rapid separation of blood plasma exosomes from low-density lipoproteins via a hydrophobic interaction chromatography method on a polyester capillary-channeled polymer fiber phase, Anal. Chim. Acta 1167 (2021), 338578.

[54] K.K. Jackson, R.R. Powell, T.F. Bruce, R.K. Marcus, Rapid isolation of extracellular vesicles from diverse biofluid matrices via capillary-channeled polymer fiber solid-phase extraction micropipette tips, Analyst 146 (13) (2021) 4314–4325.

[55] K.K. Jackson, R.R. Powell, R.K. Marcus, T.F. Bruce, Comparison of the capillary-channeled polymer (C-CP) fiber spin-down tip approach to traditional methods for the isolation of extracellular vesicles from human urine, Anal. Bioanal. Chem. 414 (13) (2022) 3813–3825.

[56] K.K. Jackson, R.R. Powell, R.K. Marcus, T.F. Bruce, Comparison of the capillary-channeled polymer (C-CP) fiber spin-down tip approach to traditional methods for the isolation of extracellular vesicles from human urine, Anal. Bioanal. Chem. 414 (13) (2022) 3813–3825.

[57] X. Ji, S. Huang, T.F. Bruce, Z. Tan, D. Wang, Z. Zhu, R.K. Marcus, D.M. Lubman, A novel method of high-purity extracellular vesicle enrichment from microliter-scale human serum for proteomic analysis, Electrophoresis 42 (2021) 245–256.

[58] B. Vestad, A. Llorente, A. Neurauter, S. Phuyal, B. Kierulf, P. Kierulf, T. Skotland, K. Sandvig, K.B.F. Haug, R. Øvstebø, Size and concentration analyses of extracellular vesicles by nanoparticle tracking analysis: a variation study, J. Extracell. Vesicles 6 (1) (2017), 1344087.

[59] D. Bachurski, M. Schuldner, P.-H. Nguyen, A. Malz, K.S. Reiners, P.C. Grenzi, F. Babatz, A.C. Schauss, H.P. Hansen, M. Hallek, E. Pogge von Strandmann, Extracellular vesicle measurements with nanoparticle tracking analysis – an accuracy and repeatability comparison between NanoSight NS300 and ZetaView, J. Extracell. Vesicles 8 (1) (2019), 1596016.

[60] P. Puzar Dominkus, M. Stenovec, S. Sitar, E. Lasic, R. Zorec, A. Plemenitas, E. Zagar, M. Kreft, M. Lenassi, PKH26 labeling of extracellular vesicles: characterization and cellular internalization of contaminating PKH26 nanoparticles, Biochim. Biophys. Acta Biomembr. 1860 (6) (2018) 1350–1361.

[61] H. Zhang, D. Lyden, Asymmetric-flow field-flow fractionation technology for exomere and small extracellular vesicle separation and characterization, Nat. Protoc. 14 (4) (2019) 1027–1053.

[62] S. Sharma, M. LeClaire, J. Wohlschlegel, J. Gimzewski, Impact of isolation methods on the biophysical heterogeneity of single extracellular vesicles, Sci. Rep. 10 (1) (2020), 13327.

[63] V. Vagenende, A.X. Han, M. Mueller, B.L. Trout, Protein-associated cation clusters in aqueous arginine solutions and their effects on protein stability and size, ACS Chem. Biol. 8 (2) (2013) 416–422.

[64] V. Vagenende, M.G. Yap, B.L. Trout, Mechanisms of protein stabilization and prevention of protein aggregation by glycerol, Biochemistry 48 (46) (2009) 11084–11096.

[65] C.Y. Soo, Y. Song, Y. Zheng, E.C. Campbell, A.C. Riches, F. Gunn-Moore, S.J. Powis, Nanoparticle tracking analysis monitors microvesicle and exosome secretion from immune cells, Immunology 136 (2) (2012) 192–197.

[66] J.M. Noble, L.M. Roberts, N. Vidavsky, A.E. Chiou, C. Fischbach, M.J. Paszek, L. A. Estroff, L.F. Kourkoutis, Direct comparison of optical and electron microscopy methods for structural characterization of extracellular vesicles, J. Struct. Biol. 210 (1) (2020), 107474.

[67] E. van der Pol, F.A. Coumans, A.E. Grootemaat, C. Gardiner, I.L. Sargent, P. Harrison, A. Sturk, T.G. van Leeuwen, R. Nieuwland, Particle size distribution of exosomes and microvesicles determined by transmission electron microscopy, flow cytometry, nanoparticle tracking analysis, and resistive pulse sensing, J Thromb Haemost 12 (7) (2014) 1182–1192.

[68] C. Gardiner, Y.J. Ferreira, R.A. Dragovic, C.W. Redman, I.L. Sargent, Extracellular vesicle sizing and enumeration by nanoparticle tracking analysis, J. Extracell. Vesicles 2 (1) (2013), 19671.

[69] M. Holcar, J. Ferdin, S. Sitar, M. Tušek-Žnidarič, V. Dolžan, A. Plemenitaš, E. Žagar, M. Lenassi, Enrichment of plasma extracellular vesicles for reliable quantification of their size and concentration for biomarker discovery, Sci. Rep. 10 (1) (2020) 1–13.

[70] E. Oeyen, K. Van Mol, G. Baggerman, H. Willems, K. Boonen, C. Rolfo, P. Pauwels, A. Jacobs, K. Schildermans, W.C. Cho, I. Mertens, Ultrafiltration and size exclusion chromatography combined with asymmetrical-flow field-flow fractionation for the isolation and characterisation of extracellular vesicles from urine, J. Extracell. Vesicles 7 (1) (2018), 1490143.

[71] K.K. Jackson, R.R. Powell, R.K. Marcus, T.F. Bruce, Comparison of the capillary-channeled polymer (C-CP) fiber spin-down tip approach to traditional methods for the isolation of extracellular vesicles from human urine, Anal. Bioanal. Chem. (2022) 1–13.

[72] J. Webber, A. Clayton, How pure are your vesicles? J. Extracell. Vesicles 2 (1) (2013), 19861.
[73] M.Y. Konoshenko, E.A. Lekchnov, A.V. Vlassov, P.P. Laktionov, Isolation of extracellular vesicles: general methodologies and latest trends, BioMed Res. Int. 2018 (2018), 8545347.
[74] R.J. Lobb, M. Becker, S.W. Wen, C.S. Wong, A.P. Wiegmans, A. Leimgruber, A. Moller, Optimized exosome isolation protocol for cell culture supernatant and human plasma, J. Extracell. Vesicles 4 (1) (2015), 27031.
[75] B.J. Tauro, D.W. Greening, R.A. Mathias, H. Ji, S. Mathivanan, A.M. Scott, R. J. Simpson, Comparison of ultracentrifugation, density gradient separation, and immunoaffinity capture methods for isolating human colon cancer cell line LIM1863-derived exosomes, Methods 56 (2) (2012) 293–304.
[76] J. Kowal, G. Arras, M. Colombo, M. Jouve, J.P. Morath, B. Primdal-Bengtson, F. Dingli, D. Loew, M. Tkach, C. Thery, Proteomic comparison defines novel markers to characterize heterogeneous populations of extracellular vesicle subtypes, Proc. Natl. Acad. Sci. U. S. A. 113 (8) (2016) E968–E977.
[77] H.A. Dad, T.W. Gu, A.Q. Zhu, L.Q. Huang, L.H. Peng, Plant exosome-like nanovesicles: emerging therapeutics and drug delivery nanoplatforms, Mol. Ther. 29 (1) (2021) 13–31.